

SOLVING AN INVERSE OBSTACLE PROBLEM FOR THE WAVE EQUATION BY USING THE BOUNDARY CONTROL METHOD

LAURI OKSANEN

ABSTRACT. We introduced in [17] a method to locate discontinuities of a wave speed in dimension two from acoustic boundary measurements modelled by the hyperbolic Neumann-to-Dirichlet operator. Here we extend the method for sound hard obstacles in arbitrary dimension. We present numerical experiments with simulated noisy data suggesting that the method is robust against measurement noise.

1. INTRODUCTION

Nondestructive obstacle reconstruction through wave propagation motivates a number of mathematical problems with several applications such as medical and seismic imaging. There is a large body of literature concerning obstacle detection using time harmonic waves, and we refer the reader to the review articles [8, 19] and to the monograph [13]. Recently there has been also interest in reconstruction methods from acoustic measurements in the time domain [6, 7, 15, 16]. In this paper we present a numerical method of the latter type. We allow the background to be anisotropic and non-homogeneous but confine ourselves to the case of non-stationary acoustic waves and the scattering from sound-hard obstacles.

Let M be a compact smooth manifold with smooth boundary ∂M and let g be a smooth Riemannian metric tensor on M . Let $\Sigma \subset M^{\text{int}}$ be a compact set with nonempty interior and smooth boundary, and let $\mu \in C^\infty(M)$ be strictly positive. We consider the following wave

Date: February 21, 2022.

1991 Mathematics Subject Classification. Primary: 35R30.

Key words and phrases. inverse problems, boundary control, wave equation, obstacle detection, scattering.

equation on M ,

$$(1) \quad \begin{aligned} \partial_t^2 u(t, x) - \Delta_{g, \mu} u(t, x) &= 0, & (t, x) &\in (0, \infty) \times (M \setminus \Sigma), \\ \partial_{\nu, \mu} u(t, x) &= f(t, x), & (t, x) &\in (0, \infty) \times \partial M, \\ \partial_{\nu, \mu} u(t, x) &= 0, & (t, x) &\in (0, \infty) \times \partial \Sigma, \\ u|_{t=0}(x) &= 0, \quad \partial_t u|_{t=0}(x) = 0, & x &\in M \setminus \Sigma, \end{aligned}$$

where $\Delta_{g, \mu}$ is the weighted Laplace-Beltrami operator and $\partial_{\nu, \mu}$ is the normal derivative corresponding to $\Delta_{g, \mu}$. That is, if we let $(g^{jk}(x))_{j,k=1}^n$ and $|g(x)|$ denote the inverse and determinant of $g(x)$ in local coordinates, then we have

$$\begin{aligned} \Delta_{g, \mu} u &= \mu^{-1} \operatorname{div}(\mu \operatorname{grad} u) \\ &= \sum_{j,k=1}^n \mu(x)^{-1} |g(x)|^{-\frac{1}{2}} \frac{\partial}{\partial x^j} \left(\mu(x) |g(x)|^{\frac{1}{2}} g^{jk}(x) \frac{\partial u}{\partial x^k} \right), \\ \partial_{\nu, \mu} u &= \mu(\operatorname{grad} u, \nu)_{TM \times T^*M} = \sum_{j,k=1}^n \mu(x) \nu_k(x) g^{jk}(x) \frac{\partial u}{\partial x^j}, \end{aligned}$$

where $\nu = (\nu_1, \dots, \nu_n)$ is the exterior co-normal vector of ∂M normalized with respect to g , that is, $\sum_{j,k=1}^n g^{jk} \nu_j \nu_k = 1$.

Let us denote the solution of (1) by $u^f(t, x) = u(t, x)$. For $T > 0$ and an open $\Gamma \subset \partial M$ we define the operator

$$\Lambda_{T, \Gamma} : f \mapsto u^f|_{(0, T) \times \Gamma}, \quad f \in C_0^\infty((0, T) \times \Gamma).$$

The Neumann-to-Dirichlet operator $\Lambda_{T, \Gamma}$ models boundary measurements with acoustic sources and receivers on Γ . Let us assume that the metric tensor g and the weight function μ are known but Σ is unknown. We consider a method to locate Σ from the measurements $\Lambda_{T, \Gamma}$.

Let us point out that if $M \subset \mathbb{R}^n$, $g = c(x)^{-2} dx^2$ and $\mu(x) = c(x)^{n-2}$ where $c \in C^\infty(M)$ is strictly positive, then $\Delta_{g, \mu} = c(x)^2 \Delta$, where Δ is the Euclidean Laplacian. Thus the isotropic wave equation,

$$\partial_t^2 u - c(x)^2 \Delta u = 0,$$

is covered by the theory. The more general equation (1) allows for an anisotropic wave speed to be modelled.

1.1. Statement of the results. Notice that the operator $\Delta_{g, \mu}$ with the domain $H^2(M) \cap H_0^1(M)$ is self-adjoint on the space $L^2(M; \mu dV_g)$, where dV_g is the Riemannian volume measure of (M, g) , that is, $\mu dV_g = \mu |g|^{1/2} dx$ in local coordinates. We call μdV_g the measure corresponding to $\Delta_{g, \mu}$ and denote it also by V .

We define for a function $\tau : \partial M \rightarrow \mathbb{R}$ the *domain of influence* with and without the obstacle,

$$\begin{aligned} M_\Sigma(\tau) &:= \{x \in M \setminus \Sigma; \text{ there is } y \in \partial M \text{ such that } d_\Sigma(x, y) \leq \tau(y)\}, \\ M(\tau) &:= \{x \in M; \text{ there is } y \in \partial M \text{ such that } d(x, y) \leq \tau(y)\}, \end{aligned}$$

where d_Σ is the Riemannian distance function of $(M \setminus \Sigma, g)$ and d is that of (M, g) . As (M, g) is known, we can compute the shape of the domain of influence $M(\tau)$ for any $\tau : \partial M \rightarrow \mathbb{R}$. Our main theorem is the following:

Theorem 1. *Let $T > 0$ and let $\Gamma \subset \partial M$ be open. For a function τ in*

$$C_T(\Gamma) := \{\tau : \partial M \rightarrow \mathbb{R}; \tau|_{\bar{\Gamma}} \in C(\bar{\Gamma}), 0 \leq \tau \leq T, \tau|_{\partial M \setminus \bar{\Gamma}} = 0\},$$

the volume $V(M_\Sigma(\tau))$ can be computed from $\Lambda_{2T, \Gamma}$ by solving a sequence of linear equations on $L^2((0, T) \times \Gamma)$. Moreover,

$$(2) \quad M(\tau)^{int} \cap \Sigma^{int} \neq \emptyset \quad \text{if and only if} \quad V(M_\Sigma(\tau)) < V(M(\tau)).$$

Theorem 1 allows us to probe the obstacle with the known domains of influence $M(\tau)$, $\tau \in C_T(\Gamma)$. We will illustrate this probing method in Section 3 via numerical experiments in the two dimensional case.

In Section 2 we give a proof of Theorem 1 that is based on ideas from the boundary control method. By using the boundary control method, a smooth wave speed can be fully reconstructed from the Neumann-to-Dirichlet operator. This uniqueness result is by Belishev [1] in the isotropic case and by Belishev and Kurylev [3] in the anisotropic case. We refer to the monograph [12] and to the review article [2] for further details on the boundary control method. The boundary control method depends on Tataru's hyperbolic unique continuation result [20], whence it is expected to have only logarithmic type stability. Also our result depends on [20], however, we overcome the ill-posedness of the reconstruction problem by regularizing it carefully. The regularization strategy is a modification of that in [4], and the iterative time-reversal control method introduced there can be adapted to give an efficient implementation of our method.

2. PROOF OF THE MAIN THEOREM

We begin by showing that the volumes $V(M_\Sigma(\tau))$, $\tau \in C_T(\Gamma)$, can be computed from $\Lambda_{2T, \Gamma}$ by solving a sequence of linear equations on $L^2((0, T) \times \partial M)$. Our proof relies on general results from regularization theory and it can also be adapted to simplify the arguments in [18]. We define the operator

$$K := J\Lambda_{2T, \Gamma}\Theta_{2T} - R\Lambda_{T, \Gamma}RJ\Theta_{2T},$$

where Θ_{2T} is the extension by zero from $(0, T)$ to $(0, 2T)$, R is the time reversal on $(0, T)$, that is $Rf(t) := f(T - t)$, and

$$Jf(t) := \frac{1}{2} \int_t^{2T-t} f(s) ds, \quad f \in L^2(0, 2T), \quad t \in (0, T).$$

We recall K is a compact operator on $L^2((0, T) \times \Gamma)$ since, see [21],

$$\Lambda_{T,\Gamma} : L^2((0, T) \times \Gamma) \rightarrow H^{2/3}((0, T) \times \Gamma).$$

Let $f \in C_0^\infty((0, T) \times \Gamma)$ and let $\phi \in C^\infty(M \setminus \Sigma)$. Moreover, let $t \in (0, \infty)$ and integrate by parts

$$(3) \quad \begin{aligned} \partial_t^2(u^f(t), \phi)_{L^2(M \setminus \Sigma; dV)} &= (\Delta_{g,\mu} u^f(t), \phi)_{L^2(M \setminus \Sigma; dV)} \\ &= -(\text{grad } u^f(t), \text{grad } \phi)_{L^2(M \setminus \Sigma; dV)} + (\partial_{\nu,\mu} u^f(t), \phi)_{L^2(\partial M; dS_g)}, \end{aligned}$$

where dS_g denotes the Riemannian surface measure on $(\partial M, g)$. Notice that the boundary term on $\partial \Sigma$ vanish as u^f satisfies the homogeneous Neumann boundary condition there.

In particular, for $f, h \in C_0^\infty((0, T) \times \Gamma)$, $t \in (0, T)$ and $s \in (0, 2T)$,

$$\begin{aligned} &(\partial_t^2 - \partial_s^2)(u^f(t), u^h(s))_{L^2(M \setminus \Sigma; dV)} \\ &= (f(t), \Lambda_{2T,\Gamma} h(s))_{L^2(\partial M; dS_g)} - (\Lambda_{T,\Gamma} f(t), h(s))_{L^2(\partial M; dS_g)}. \end{aligned}$$

By solving this wave equation with vanishing initial conditions at $t = 0$ and noticing that $\Lambda_{T,\Gamma}^* = R\Lambda_{T,\Gamma}R$, we get the Blagoveščenskiĭ's identity

$$(4) \quad (u^f(T), u^h(T))_{L^2(M \setminus \Sigma; dV)} = (f, Kh)_{L^2((0,T) \times \Gamma; dt \otimes dS_g)},$$

that holds for all $f, h \in L^2((0, T) \times \Gamma)$ by continuity of K and density of smooth functions in L^2 . The identity (4) originates from [5].

Moreover, by letting $\phi = 1$ identically in (3), we get

$$(5) \quad \partial_t^2(u^f(t), 1)_{L^2(M \setminus \Sigma; dV)} = (\partial_{\nu,\mu} u^f(t), 1)_{L^2(\partial M; dS_g)}.$$

Notice that this identity does not hold if u^f satisfies the homogeneous Dirichlet boundary condition on $\partial \Sigma$, instead of the Neumann one. This is why our method does not extend to detection of sound soft obstacles in a straightforward manner. We get the identity

$$(6) \quad (u^f(T), 1)_{L^2(M \setminus \Sigma; dV)} = (f, b)_{L^2((0,T) \times \Gamma; dt \otimes dS_g)},$$

where $b(t, x) = T - t$, by solving the ordinary differential equation (5) with vanishing initial conditions at $t = 0$.

Let $\tau \in C_T(\Gamma)$ and let us define the set

$$S_\tau := \{(t, x) \in [0, T] \times \bar{\Gamma}; \quad t \in [T - \tau(x), T]\}.$$

We define the operator

$$W_\tau f := u^f(T), \quad W_\tau : L^2(S_\tau) \rightarrow L^2(M \setminus \Sigma).$$

It follows from [14] that W_τ is compact. Moreover, we may consider a restriction of K ,

$$K_\tau f = Kf|_{S_\tau}, \quad K_\tau : L^2(S_\tau) \rightarrow L^2(S_\tau).$$

Then the equations (4) and (6) yield that on $L^2(S_\tau)$

$$(7) \quad W_\tau^* W_\tau = K_\tau, \quad W_\tau^* 1 = b.$$

Let us now consider the control equation,

$$(8) \quad W_\tau f = 1, \quad \text{for } f \in L^2(S_\tau).$$

We have $\text{supp}(W_\tau f) \subset M_\Sigma(\tau)$ since the wave equation (1) has finite speed of propagation. Moreover, it can be shown using Tataru's unique continuation [20] that the inclusion

$$(9) \quad \{W_\tau f; f \in L^2(S_\tau)\} \subset L^2(M_\Sigma(\tau)),$$

is dense, see the appendix below. In particular, if there is a least squares solution f_0 to (8) then $W_\tau f_0 = 1_{M_\Sigma(\tau)}$. However, as W_τ is compact, the range of W_τ is a proper dense subset of $L^2(M_\Sigma(\tau))$ and (8) may fail to have a least squares solution. Nonetheless, it is instructive to consider first the case where (8) has a least squares solution. Then the least squares solution of minimal norm f_0 is given by the pseudoinverse, see e.g. [9, Th. 2.6],

$$f_0 = W_\tau^\dagger 1 = (W_\tau^* W_\tau)^\dagger W_\tau^* 1 = K_\tau^\dagger b,$$

and we can compute the volume $V(M_\Sigma(\tau))$ from the boundary data $\Lambda_{2T, \Lambda}$ by the formula

$$\begin{aligned} V(M_\Sigma(\tau)) &= (1_{M_\Sigma(\tau)}, 1)_{L^2(M \setminus \Sigma; dV)} = (W_\tau W_\tau^\dagger 1, 1)_{L^2(M \setminus \Sigma; dV)} \\ &= (K_\tau^\dagger b, b)_{L^2(S_\tau; dt \otimes dS_g)}. \end{aligned}$$

The standard technique to remedy the nonexistence of a least squares solution to a linear equation is to use a regularization method. As W_τ is compact and we have the information (7) at our disposal, there are several ways to regularize that are available to us. For example, we could use a regularization by projection [9, Section 3.3] or a regularization based on a spectral approximation of the inverse [9, Th. 4.1]. Here we will consider only the classical Tikhonov regularization,

$$(10) \quad f_\alpha := (W_\tau^* W_\tau + \alpha)^{-1} W_\tau^* 1 = (K_\tau + \alpha)^{-1} b, \quad \alpha > 0.$$

We have the following abstract lemma.

Lemma 1. *Suppose that X and Y are Hilbert spaces. Let $y \in Y$ and let $A : X \rightarrow Y$ be a bounded linear operator with the range $R(A)$.*

Then $Ax_\alpha \rightarrow Py$ as $\alpha \rightarrow 0$, where $x_\alpha = (A^*A + \alpha)^{-1}A^*y$, $\alpha > 0$, and $P : Y \rightarrow \overline{R(A)}$ is the orthogonal projection.

Proof. Notice that for all $x \in X$

$$\|Ax - y\|^2 = \|Ax - Py\|^2 + \|(1 - P)y\|^2.$$

By [9, Th. 5.1] we know that x_α is the unique minimizer of

$$\|Ax - y\|^2 + \alpha \|x\|^2.$$

Let $\epsilon > 0$ and let $x^\epsilon \in X$ satisfy $\|Ax^\epsilon - Py\|^2 < \epsilon$. Then

$$\begin{aligned} \|Ax_\alpha - Py\|^2 &= \|Ax_\alpha - y\|^2 - \|(1 - P)y\|^2 \\ &\leq \|Ax_\alpha - y\|^2 + \alpha \|x_\alpha\|^2 - \|(1 - P)y\|^2 \\ &\leq \|Ax^\epsilon - y\|^2 + \alpha \|x^\epsilon\|^2 - \|(1 - P)y\|^2 \\ &= \|Ax^\epsilon - Py\|^2 + \alpha \|x^\epsilon\|^2 < \epsilon + \alpha \|x^\epsilon\|^2 \leq 2\epsilon, \end{aligned}$$

for $\alpha \leq \epsilon / \|x^\epsilon\|^2$. \square

By the density (9) we have that $\overline{R(W_\tau)} = L^2(M_\Sigma(\tau))$. Thus the above lemma implies that $Wf_\alpha \rightarrow 1_{M_\Sigma(\tau)}$ in $L^2(M \setminus \Sigma)$ as α tends to zero. In particular, we may compute the volume $V(M_\Sigma(\tau))$ from the boundary data $\Lambda_{2T, \Lambda}$ by the formula

$$(11) \quad V(M_\Sigma(\tau)) = \lim_{\alpha \rightarrow 0^+} ((K_\tau + \alpha)^{-1}b, b)_{L^2(S_\tau; dt \otimes dS_g)}.$$

Lemma 2. *Let $T > 0$, $\Gamma \subset \partial M$ be open and let $\tau \in C_T(\Gamma)$. Then*

$$M(\tau)^{\text{int}} \cap \Sigma^{\text{int}} \neq \emptyset \quad \text{if and only if} \quad V(M_\Sigma(\tau)) < V(M(\tau)).$$

Proof. Notice that $d_\Sigma(x, y) \geq d(x, y)$ for any $x, y \in M \setminus \Sigma$. Hence $M_\Sigma(\tau) \subset M(\tau)$. Moreover, $M_\Sigma(\tau) \cap \Sigma = \emptyset$ by definition. In particular, if the open set $M(\tau)^{\text{int}} \cap \Sigma^{\text{int}}$ is nonempty, then

$$\begin{aligned} V(M_\Sigma(\tau)) &\leq V(M(\tau) \setminus \Sigma) \\ &< V(M(\tau) \setminus \Sigma) + V(M(\tau)^{\text{int}} \cap \Sigma^{\text{int}}) \leq V(M(\tau)). \end{aligned}$$

Thus we have shown the implication from left to right in (2).

Let us now suppose that $V(M_\Sigma(\tau)) < V(M(\tau))$. Then $M(\tau) \setminus M_\Sigma(\tau)$ is not a null set (that is, a set of measure 0). But $\partial M(\tau)$ is a null set [18], whence there is $x \in M(\tau)^{\text{int}} \setminus M_\Sigma(\tau)$. Thus there is $y \in \partial M$ and a path $\gamma : [0, \ell] \rightarrow M$ from y to x such that the length of γ satisfies $l(\gamma) \leq \tau(y)$. The path γ intersects Σ since otherwise we would have $x \in M_\Sigma(\tau)$. Let $z \in \Sigma \cap \gamma([0, \ell])$. Then $z \in M(\tau)^{\text{int}}$ since $x \in M(\tau)^{\text{int}}$, and there is a neighborhood $U \subset M(\tau)^{\text{int}}$ of z such that $U \cap \Sigma^{\text{int}} \neq \emptyset$. Hence also $M(\tau)^{\text{int}} \cap \Sigma^{\text{int}} \neq \emptyset$. \square

Theorem 1 follows from the formula (11) and Lemma 2.

3. NUMERICAL RESULTS

3.1. Simulation of the data. In all our numerical examples (M, g) is the two-dimensional unit square with the Euclidean metric, that is,

$$M = [0, 1]^2, \quad g = (dx^1)^2 + (dx^2)^2.$$

Moreover, $T = 1$ and the accessible part of the boundary Γ is the bottom edge of M ,

$$\Gamma = \{(x^1, 0) \in M; x^1 \in (0, 1)\}.$$

For computation of the Dirichlet-to-Neumann map we discretize in space by using finite elements, and solve the resulting system of ordinary differential equations by a backward differentiation formula (BDF). To be very specific, we use the commercial Comsol solver with quadratic Lagrange elements and BDF time-stepping with maximum order of 2. Both the maximum element size and time step size are set to the constant value $h = 0.0025$.

We discretize the measurement $\Lambda_{\Gamma, 2T}f$, $f \in L^2((0, T) \times \Gamma)$, by taking the point values on the uniform grid of temporal points $t_j \in [0, 2T]$, $j = 1, 2, \dots, N_t$, and spatial points $x_k \in \Gamma$, $k = 1, 2, \dots, N_x$, where $N_x = 20$ and $N_t = 800$. The higher precision in time reflects the fact that a measurement of this type can be realized by using N_x receivers (e.g. microphones) with the sampling rate h .

We model noisy measurements by adding white Gaussian noise to the signal

$$\lambda_f(j, k) := \Lambda_{\Gamma, T}f(t_j, x_k), \quad j = 1, 2, \dots, N_t, \quad k = 1, 2, \dots, N_x.$$

To be very specific, we use the Matlab function `awgn` both to measure the power of the signal λ_f and to add noise with specified signal-to-noise ratio (SNR). We have used signal-to-noise ratios $14dB$ and $7dB$ corresponding to 4% and 20% noise power levels.

3.2. Solving the control equation. The operator K_τ is self-adjoint and positive-semidefinite by (7), whence $K_\tau + \alpha$ positive-definite for $\alpha > 0$. We solve the Tikhonov regularized control equation

$$(12) \quad (K_\tau + \alpha)f = b$$

by using the conjugate gradient (CG) method on a finite dimensional subspace $\mathcal{C}_\tau \subset L^2(S_\tau)$ that we will define below. We have used the initial value $f = 0$ in all our CG iterations.

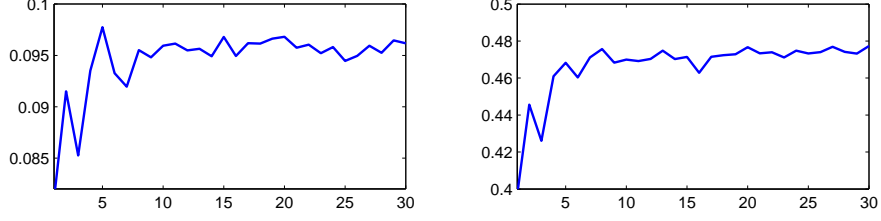


FIGURE 1. Convergence of the reconstructed volume $V(M_\emptyset(\tau_r))$ as a function of N_{cg} , i.e. the number of the conjugate gradient steps. Noiseless case. *Left:* $r = 1/10$; *right:* $r = 1/2$.

We denote by $\Gamma_k \subset \Gamma$ the Voronoi cell corresponding to the measurement point x_k , $k = 1, 2, \dots, N_x$, that is,

$$\Gamma_k := \{x \in \Gamma; |x - x_k| \leq |x - x_l|, \quad l = 1, 2, \dots, N_x\}.$$

Moreover, we denote by \mathcal{C} the space of piecewise constant sources f that can be represented as a linear combination of the functions

$$(13) \quad f_k(t, x) := 1_{[0, h]}(t) 1_{\Gamma_k}(x), \quad k = 1, 2, \dots, N_x,$$

and their time translations by an integer multiple of h . Finally, we define

$$\mathcal{C}_\tau := \{f \in \mathcal{C}; \text{supp}(f) \subset S_\tau\}, \quad \tau \in C_T(\Gamma).$$

As the wave equation (1) is invariant with respect to translations in time, we can compute λ_f for arbitrary $f \in \mathcal{C}_\tau$ and $\tau \in C_T(\Gamma)$ if we are given the measurements

$$\lambda_{f_k}, \quad k = 1, 2, \dots, N_x.$$

To summarize, we employ $N_x = 20$ measurements that can be realized by using N_x receivers with the sampling rate $h = 0.0025$.

3.3. Regularization and calibration. As the control equation (12) may be ill-posed for $\alpha = 0$, we terminate the CG iteration early after N_{cg} steps. This amounts to regularization of the problem [10]. To calibrate the method we probed the empty space case, $\Sigma = \emptyset$, with half-spaces. That is, we chose the profile function $\tau \in C_T(\Gamma)$ to be of the form,

$$\tau_r(x) := r, \quad x \in \Gamma, \quad r \in [1/10, 1/2].$$

In this case, the CG iteration essentially converges after 10 steps even when not using the Tikhonov regularization, that is, $\alpha = 0$, see Figure 1. For this reason, we have chosen $N_{cg} = 10$ in all our further simulations.

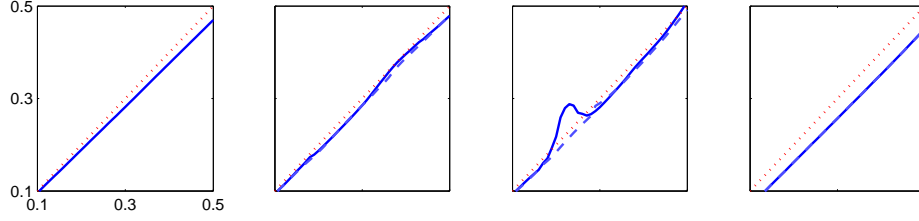


FIGURE 2. Reconstructed volumes $V(M_\emptyset(\tau_r))$ as a function of r compared to the real volume (dotted red). The two reconstructions (solid blue and dashed blue) correspond to two different realizations of noise. *From left, 1st:* noiseless, $\alpha = 0$; *2nd:* SNR = 14dB, $\alpha = 0$; *3rd:* SNR = 7dB, $\alpha = 0$; *4th:* SNR = 7dB, $\alpha = 10^{-3}$.

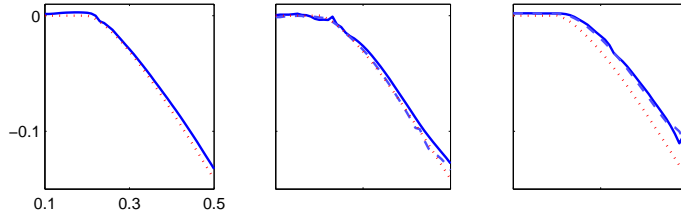


FIGURE 3. Reconstructed volume differences (14) with $\tau = \tau_r$ as a function of r compared to the real difference (dotted red) in the case of the disk shaped obstacle $\Sigma = \Sigma_\circ$. The two reconstructions (solid blue and dashed blue) correspond to two different realizations of noise. *From left, 1st:* noiseless, $\alpha = 0$; *2nd:* SNR = 14dB, $\alpha = 0$; *3rd:* SNR = 7dB, $\alpha = 10^{-3}$.

In addition to the empty space case, we have experimented with the disk and the square shaped obstacles defined as follows: Σ_\circ is the disk with radius $3/10$ and center $p := (1/2, 1/2)$ and Σ_\diamond is the square with side length 0.424 , center p and axes rotated by $\pi/4$ with respect to the axes of M , see Figure 4.

It is not clear to us, why the method underestimates the volume $V(M_\emptyset(\tau_r))$, see Figure 2 (leftmost plot). One possibility is that we using too few spatial basis functions, however, the smallness of N_x is motivated by applications. Moreover, the underestimation is systematic and is canceled when considering the volume differences,

$$(14) \quad V(M_\Sigma(\tau)) - V(M_\emptyset(\tau)),$$

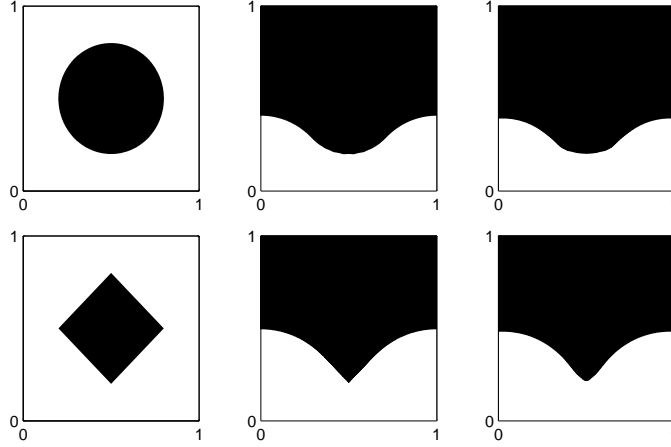


FIGURE 4. *Top row from left, 1st:* The disk shaped obstacle $\Sigma = \Sigma_{\circ}$. *2nd:* The largest region on which the absence of the obstacle can be concluded when probing with disk shaped domains of influence $H_{\Sigma_{\circ}}(\Gamma)$. *3rd:* A reconstruction of $H_{\Sigma_{\circ}}(\Gamma)$ in the noiseless case. The threshold $\epsilon = 5/10^4$. *Bottom row:* The square shaped obstacle $\Sigma = \Sigma_{\diamond}$, $H_{\Sigma_{\diamond}}(\Gamma)$ and a reconstruction of $H_{\Sigma_{\diamond}}(\Gamma)$. The same parameter values are used for both the reconstructions.

see Figure 3. In terms of applications, this means that we should calibrate the method in a known background before probing a region that possibly contains an obstacle.

According to our experiments the method reconstructs volumes reliably when $\text{SNR} = 14\text{dB}$ and we regularize only through the early termination of the CG iteration. When $\text{SNR} = 7\text{dB}$ and $\alpha = 0$, a reconstruction can be seriously disrupted even in the empty space case. After introducing Tikhonov regularization with $\alpha = 10^{-3}$, the effect of noise vanishes but a large systematic error appears, see Figure 2 (the two rightmost plots). We see that considering the volume differences (14) becomes even more essential when $\alpha > 0$.

3.4. Probing with disk shaped domains of influence. We will now describe our experiments concerning reconstruction of the shape of an obstacle. To this purpose, we chose the profile function $\tau \in C_T(\Gamma)$ to be of the form,

$$\tau_r^y(x) := r - |x - y|, \quad x \in \Gamma, \quad y \in \Gamma, \quad r \in [1/10, 1/2].$$

Then $M(\tau_r^y) = \overline{B(y, r)} \cap M$, that is, the intersection of M and the closed disk of radius r centered at y . Probing with disks has been

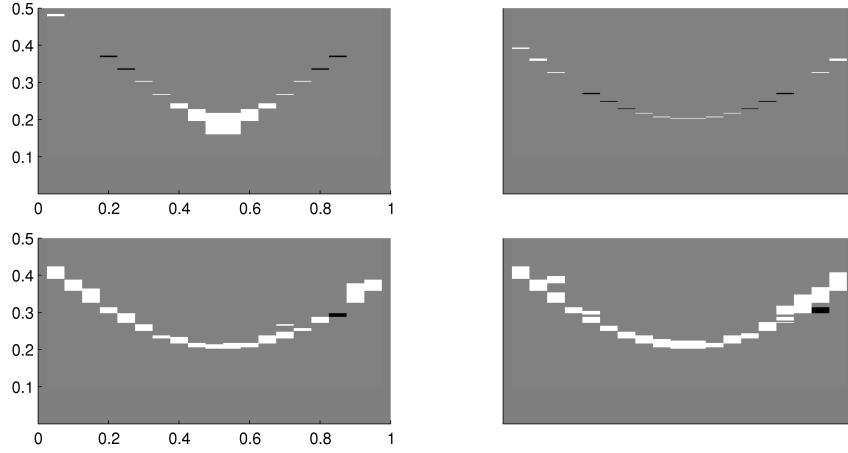


FIGURE 5. Comparison of a reconstruction $\tilde{H}_\Sigma(\Gamma)$ with the theoretical best possible reconstruction $H_\Sigma(\Gamma)$. Erroneous pixels in $\tilde{H}_\Sigma(\Gamma) \setminus H_\Sigma(\Gamma)$ are drawn in white and $H_\Sigma(\Gamma) \setminus \tilde{H}_\Sigma(\Gamma)$ in black. Gray pixels are reconstructed correctly. *Top row:* Noiseless measurements with the threshold $\epsilon = 5/10^4$, *left:* $\Sigma = \Sigma_\circ$; *right:* $\Sigma = \Sigma_\circ$. *Bottom row:* SNR = 14dB, $\Sigma = \Sigma_\circ$ and $\epsilon = 4/10^3$. The two reconstructions correspond to two different realizations of noise.

considered in the context of electrical impedance tomography in [11] and our numerical results are comparable to the results therein.

Analogously to [11] and [17], let us define the largest region $H_\Sigma(\Gamma)$ on which we can conclude the absence of obstacles by probing with the sets $\overline{B(y, r)} \cap M$, $y \in \Gamma$, $r \in (0, T]$. We denote

$$\begin{aligned} R_T(y) &:= \sup\{r \in (0, T]; B(y, r) \cap \Sigma^{\text{int}} = \emptyset\} \\ &= \sup\{r \in (0, T]; V(M_\Sigma(\tau_r^y)) = V(M(\tau_r^y))\}, \end{aligned}$$

and define

$$H_\Sigma(\Gamma) := \bigcup_{y \in \Gamma} (B(y, R_T(y)) \cap M).$$

Let us describe next how we approximate $R_T(y)$ when computing with finite precision. Let $\epsilon > 0$, $N_r \in \mathbb{N}$ and let $r_l \in [0, T]$, $l = 1, 2, \dots, N_r$, be a uniform grid of points. We denote

$$L(\epsilon, N_r) := \max\{l = 1, 2, \dots, N_r; V(M_\Sigma(\tau_r^y)) - V(M_\emptyset(\tau_r^y)) \geq -\epsilon\},$$

and define the approximation $r_T(y; \epsilon, N_r) = r_{L(\epsilon, N_r)}$ of $R_T(y)$. We have used the threshold $\epsilon = 5/10^4$ in noiseless cases and $\epsilon = 4/10^3$ when SNR = 14dB. According to our numerical experiments the method

reconstructs $H_\Sigma(\Gamma)$ reliably when using these values of ϵ and $N_r = 500$, see Figure 5, where a white pixel means that the center point of the pixel is erroneously identified to be in $H_\Sigma(\Gamma)$ (false positive) and a black pixel means erroneous identification of not being in $H_\Sigma(\Gamma)$ (false negative).

Computationally the shape reconstruction amounts to solving a large number of independent systems of linear equations by running a few number of CG steps for each of them. Our implementation with parameters as above and r_l 's restricted in $[1/10, 1/2]$ led to 4020 systems with the number of unknowns varying between 30 and 1000. The run time for the full reconstruction on a single processor was about 10 minutes, however, as the systems are independent, the method allows for an efficient parallel implementation.

APPENDIX: APPROXIMATE CONTROLLABILITY

In this section we show that the inclusion (9) is dense, that is we prove the following lemma.

Lemma 3. *Let $T > 0$, let $\Gamma \subset \partial M$ be open and let $\tau \in C_T(\Gamma)$. Then*

$$(15) \quad \{u^f(T); f \in C_0^\infty(S_\tau)\}$$

is dense in $L^2(M_\Sigma(\tau))$.

A density result of this type is called approximate controllability in the control theoretic literature. To our knowledge, Lemma 3 is proved previously only in the case of a constant function τ , see e.g. [12, Th. 3.10]. We will give a proof in the general case $\tau \in C_T(\Gamma)$ by reducing it to the constant function case. To simplify the notation we consider only the case $\Sigma = \emptyset$, since the general case follows by replacing M by $M \setminus \Sigma$ in the proofs below.

Lemma 4. *Let $T > 0$, $J \in \mathbb{N}$, let $\Gamma_j \subset \partial M$ be open and let $h_j \in C_T(\Gamma_j)$ for $j = 1, 2, \dots, J$. We define*

$$(16) \quad h^J(y) := \begin{cases} \max\{h_j(y); j \text{ satisfies } \bar{\Gamma}_j \ni y\}, & y \in \bigcup_{j=1}^J \bar{\Gamma}_j, \\ 0, & \text{otherwise.} \end{cases}$$

If for all $j = 1, \dots, J$ the functions (15) for $\tau = h_j$ are dense in $L^2(M(h_j))$, then the functions (15) for $\tau = h^J$ are dense in $L^2(M(h^J))$.

Proof. Notice that $\partial M \subset M(\tau)$ if $\tau(y) \geq 0$ for all $y \in \partial M$. Abusing the notation slightly, we will consider $M(\tau)$ as a subset of M^{int} . This does not affect the density since ∂M is a null set. We denote $\Gamma^J := \bigcup_{j=1}^J \Gamma_j$

and have

$$\begin{aligned}
 M(h^J) &= \{x \in M^{\text{int}}; \text{ there is } y \in \bar{\Gamma}^J \text{ s.t. } d(x, y) \leq h(y)\} \\
 &= \bigcup_{j=1}^J \{x \in M^{\text{int}}; \text{ there is } y \in \bar{\Gamma}_j \text{ s.t. } d(x, y) \leq h_j(y)\} \\
 &= \bigcup_{j=1}^J M(\Gamma_j, h_j).
 \end{aligned}$$

We will now prove the density by induction with respect to J . The case $J = 1$ is trivial. Let us denote $M_0 := M(h^J)$ and $M_1 := M(h_{J+1})$. Let $\psi \in L^2(M_0 \cup M_1)$. By induction hypothesis there is a sequence of smooth functions $(f_k^0)_{k=1}^\infty$ supported in S_{h^J} such that

$$u^{f_k^0}(T) \rightarrow 1_{M_0}\psi.$$

Moreover, there is a sequence of smooth functions $(f_k^1)_{k=1}^\infty$ supported in $S_{h_{J+1}}$ such that

$$u^{f_k^1}(T) \rightarrow 1_{M_1}(\psi - 1_{M_0}\psi).$$

Thus

$$\begin{aligned}
 u^{f_k^0 + f_k^1}(T) &\rightarrow 1_{M_0}(1 - 1_{M_1})\psi + 1_{M_1}\psi = (1_{M_0 \setminus M_1} + 1_{M_1})\psi \\
 &= 1_{M_0 \cup M_1}\psi = \psi.
 \end{aligned}$$

Moreover, $f_k^0 + f_k^1$ is supported in $S_{h^J} \cup S_{h_{J+1}} \subset S_{h^{J+1}}$. \square

Proof of Lemma 3. Let $\psi \in L^2(M(\tau))$ and $\epsilon > 0$. There is a simple function

$$h_\epsilon(y) = \sum_{j=1}^J T_j 1_{\Gamma_j}(y),$$

where $J \in \mathbb{N}$, $T_j \in (0, T)$ and $\Gamma_j \subset \Gamma$ are open and disjoint, such that $\tau < h_\epsilon + \epsilon$ almost everywhere on Γ and $h_\epsilon < \tau$ on $\bar{\Gamma}$, see e.g. [18, proof of Lem. 4.2]. We denote $h_j := T_j 1_{\bar{\Gamma}_j}$ and define $\tau_\epsilon = h^J$ as the maximum (16). By the construction $\tau_\epsilon < \tau$ and $\tau_\epsilon \geq h_\epsilon$.

The functions (15) for $\tau = h_j$ are dense in $L^2(M(h_j))$ by [12, proof of Th. 3.10]. Lemma 4 implies that there is a smooth function f supported in $S_{\tau_\epsilon} \subset S_\tau$ such that

$$\|1_{M(\tau_\epsilon)}\psi - u^f(T)\|_{L^2(M)}^2 < \epsilon.$$

Thus

$$(17) \quad \|\psi - u^f(T)\|_{L^2(M)}^2 < \epsilon + \int_{M(\tau) \setminus M(\tau_\epsilon)} \psi^2 dV.$$

We have $V(M(\tau_\epsilon)) \rightarrow V(M(\tau))$ as $\epsilon \rightarrow 0$, see [18]. Thus the second term in (17) tends to zero as $\epsilon \rightarrow 0$. \square

Acknowledgements. The research was supported by Finnish Centre of Excellence in Inverse Problems Research, Academy of Finland project COE 250215, and by European Research Council advanced grant 400803.

REFERENCES

- [1] M. I. Belishev. An approach to multidimensional inverse problems for the wave equation. *Dokl. Akad. Nauk SSSR*, 297(3):524–527, 1987.
- [2] M. I. Belishev. Recent progress in the boundary control method. *Inverse Problems*, 23(5):R1–R67, 2007.
- [3] M. I. Belishev and Y. V. Kurylev. To the reconstruction of a Riemannian manifold via its spectral data (BC-method). *Comm. Partial Differential Equations*, 17(5-6):767–804, 1992.
- [4] K. Bingham, Y. Kurylev, M. Lassas, and S. Siltanen. Iterative time-reversal control for inverse problems. *Inverse Probl. Imaging*, 2(1):63–81, 2008.
- [5] A. S. Blagoveščenskii. The inverse problem of the theory of seismic wave propagation. In *Problems of mathematical physics, No. 1: Spectral theory and wave processes (Russian)*, pages 68–81. (errata insert). Izdat. Leningrad. Univ., Leningrad, 1966.
- [6] C. Burkard and R. Potthast. A time-domain probe method for three-dimensional rough surface reconstructions. *Inverse Probl. Imaging*, 3(2):259–274, 2009.
- [7] Q. Chen, H. Haddar, A. Lechleiter, and P. Monk. A sampling method for inverse scattering in the time domain. *Inverse Problems*, 26(8):085001, 17, 2010.
- [8] D. Colton, J. Coyle, and P. Monk. Recent developments in inverse acoustic scattering theory. *SIAM Rev.*, 42(3):369–414 (electronic), 2000.
- [9] H. W. Engl, M. Hanke, and A. Neubauer. *Regularization of inverse problems*, volume 375 of *Mathematics and its Applications*. Kluwer Academic Publishers Group, Dordrecht, 1996.
- [10] M. Hanke. *Conjugate gradient type methods for ill-posed problems*, volume 327 of *Pitman Research Notes in Mathematics Series*. Longman Scientific & Technical, Harlow, 1995.
- [11] T. Ide, H. Isozaki, S. Nakata, S. Siltanen, and G. Uhlmann. Probing for electrical inclusions with complex spherical waves. *Comm. Pure Appl. Math.*, 60(10):1415–1442, 2007.
- [12] A. Katchalov, Y. Kurylev, and M. Lassas. *Inverse boundary spectral problems*, volume 123 of *Chapman & Hall/CRC Monographs and Surveys in Pure and Applied Mathematics*. Chapman & Hall/CRC, Boca Raton, FL, 2001.

- [13] A. Kirsch and N. Grinberg. *The factorization method for inverse problems*, volume 36 of *Oxford Lecture Series in Mathematics and its Applications*. Oxford University Press, Oxford, 2008.
- [14] I. Lasiecka and R. Triggiani. Regularity theory of hyperbolic equations with nonhomogeneous Neumann boundary conditions. II. General boundary data. *J. Differential Equations*, 94(1):112–164, 1991.
- [15] C. D. Lines and S. N. Chandler-Wilde. A time domain point source method for inverse scattering by rough surfaces. *Computing*, 75(2-3):157–180, 2005.
- [16] D. R. Luke and R. Potthast. The point source method for inverse scattering in the time domain. *Math. Methods Appl. Sci.*, 29(13):1501–1521, 2006.
- [17] L. Oksanen. Inverse obstacle problem for the non-stationary wave equation with an unknown background. *preprint, arXiv:1106.3204*, June 2011.
- [18] L. Oksanen. Solving an inverse problem for the wave equation by using a minimization algorithm and time-reversed measurements. *Inverse Probl. Imaging*, 5(3):731–744, 2011.
- [19] R. Potthast. A survey on sampling and probe methods for inverse problems. *Inverse Problems*, 22(2):R1–R47, 2006.
- [20] D. Tataru. Unique continuation for solutions to PDE’s; between Hörmander’s theorem and Holmgren’s theorem. *Comm. Partial Differential Equations*, 20(5-6):855–884, 1995.
- [21] D. Tataru. On the regularity of boundary traces for the wave equation. *Ann. Scuola Norm. Sup. Pisa Cl. Sci. (4)*, 26(1):185–206, 1998.

UNIVERSITY OF HELSINKI, P.O. BOX 68 FI-00014
E-mail address: lauri.oksanen@helsinki.fi